Digestion Processes and Elemental Analysis of Oxide and Sulfide Solid Electrolytes

Thomas F. Malkowski[a], Ethan D. Boeding[a,b], Dina Fattakhova-Rohlfing[c,d], Nadine Wettengl[e], Martin Finsterbusch[c], Gabriel M. Veith[a,b*]

[a] Chemical Sciences Division, Oak Ridge National Laboratory, Oak Ridge Tennessee, United States

[b] Bredesen Center, University of Tennessee, Knoxville Tennessee, United States

[c] Institute of Energy and Climate Research – Materials Synthesis and Processing (IEK-1), Forschungszentrum Jülich GmbH, Wilhelm-Johnen-Str., 52425 Jülich, Germany

[d] Faculty of Engineering and Center for Nanointegration Duisburg-Essen (CENIDE), Universität Duisburg-Essen, Lotharstraße 1, 47057 Duisburg, Germany

[e] Central Institute for Engineering, Electronics and Analytics, Analytics (ZEA-3), Forschungszentrum Jülich GmbH, 52425 Jülich, Germany

[*] *Corresponding Author: veithgm@ornl.gov*

ORCID

Thomas F. Malkowski, 0000-0002-0302-0969

Ethan D. Boeding, 0000-0001-7157-4712

Dina Fattakhova-Rohlfing, 0000-0003-2008-0151

Nadine Wettengl,

Martin Finsterbusch, 0000-0001-7027-7636

Gabriel M. Veith, 0000-0002-5186-4461

Abstract

Detailed elemental analysis is essential for a successful development and optimization of material systems and synthesis methods. This is especially relevant for Li and Na containing compounds, found in state of the art and next generation battery systems. Their materials properties and thus the final device performance strongly depends on the crystal structure, the stoichiometry and defect chemistry, e.g., influencing charge carrier concentration and activation energies for vacancy transport. However, a detailed quantitative analysis of light elements in a heavy matrix, featuring a broad range of solubilities and vapor pressures, is often difficult and associated with large uncertainties and thus neglected in favor of just reporting the stoichiometry as "weighed-in". In this work we report several approaches to digest and dissolve various oxide and sulfide-based materials, used in next generation Li batteries, for elemental analysis via optical emission spectroscopy. Facile and optimized procedures to digest and dissolve the most common solid-electrolytes Li-La-Ti-O, a perovskite material (LLTO), and Li-La-Zr-O which has garnet structure (LLZO). Additionally, a facile thermal digestion process is reported for a surrogate sulfide solid electrolyte (Na_2S). The digestion procedures reported here are suitable for almost any laboratory environment and when applied, will improve understanding of the synthesis-structure-property correlations needed to advanced batteries with all solid-state configurations.

Introduction

There is an old Appalachian adage about assuming. Loosely translated, if a person were to assume they rapidly make a fool of you and me. In the field of solid electrolytes, it has become gospel that one must add an excess of Li precursor (up to 20 wt%) to the starting mixture to account for lithium losses during synthesis and processing.(*1-11*) However, it is also known that a sufficient level of Li vacancies is needed (i.e. stoichiometric composition) to achieve maximum conductivity.(*4, 12-14*) Additionally, the excess Li adds considerable cost to a material and leads to a number of heretofore unanswered questions regarding where does this excess lithium go? Are the solid electrolyte materials stoichiometric? And what processing steps can be done to optimize synthesis and composition while driving optimal ionic conductivity and transport? Without rigorous answers to these questions, reproducibility of synthesis and fabrication methods for ceramic Li-ion conductors and thus translation into industrial processes is elusive.

Unfortunately, answering these questions is challenging due to the difficulty in dissolving/digesting the materials for traditional elemental analysis through inductivity coupled plasma (ICP) or atomic adsorption (AA) spectroscopies. While some groups only report the weight of Li in amounts, assuming stoichiometric Li composition after the (various) heat treatment steps, other teams turn to techniques such as time of flight secondary ion mass spectroscopy (TOF-SIMS) or ion beam analysis when they characterize the composition.(*15*) Teams that do use optical spectroscopies often do not report the dissolution procedure

in sufficient detail to ensure reproducibility. Further, stability in the digestion media is essential to reproducible elemental analysis. To answer these questions, we have sought robust analytical procedures to digest standard solid electrolytes such as the perovskites (e.g., $Li_{0.3}La_{0.57}TiO_3$ (LLTO)), garnets (e.g., $Li_7La_3Zr_2O_{12}$ (LLZO)) and sulfides (Na_2S). In this paper, we document these findings, including error approximations and hope that it will help researchers to start answering the questions detailed above. It is important to note that the availability of ICP-optical emission systems is much more common, and the operating costs lower, and analysis simpler, compared to TOF-SIMS or ion-beam analysis instruments, making the procedures reported here easily deployable on a global scale.

Experimental

Safety Warning: For those utilizing the approaches outlined below, or other approaches of their experimental design, *extreme care* should be taken due to the chemical hazards associated with the reagents described below. This includes proper personnel protective equipment and well-defined egress routes. We highly recommend working with a partner and being free of all distractions. The data discussed below will include observations of reactions, gas evolution, and colors to aid in those implementing these procedures. There are a number of gasses evolved so the work should be performed in a fume hood with adequate ventilation.

Reagents: 18 MΩ ultrapure deionized water, HCl acid (Aristar Plus, VWR Chemicals), HNO_3 acid (Aristar Plus, VWR Chemicals), H_2SO_4 acid (trace metals grade, Fisher Chemical), H_3PO_4 acid (Alfa Aesar, 85 wt. % solution), HF acid (48 wt. % solution, Sigma Aldrich ≥99.99% trace metals basis), H_3BO_4 (Sigma Aldrich, ≥99.5%), H_2O_2 (30% Reagent Grade, Fischer Scientific – stored at 1°C), oxalic acid dihydrate (Sigma Aldrich, ACS reagent ≥99%), ammonium sulfate (Fisher Scientific, 99.9%), NaOH (Mallinckrodt, Inc. ≥98%). 1,000 mg/L ICP standards were purchased from Sigma Aldrich (TraceCERT grade). Solid electrolyte materials were made in house using standard synthesis routes describes in our previous publications(*16, 17*) or as received from Steward Advanced Materials (Chattanooga TN) – $Li_{0.3}La_{0.57}TiO_3$. Na_2S (Sigma Aldrich, ACS reagent ≥99%) was used as a surrogate for sulfide solid electrolytes.

Digestion processes:

For the oxide solid electrolytes, having an extremely high thermal stability and chemical stability, two classes of digestion processes were investigated utilizing a hot plate or a microwave. Typically, 5-50 mg of material was ground in an agate mortar before use. Powders were added first followed by the slow addition of solution. For LLZO doped with Ta (LLZTO) it was found that a mixture of H_2SO_4:HNO_3:H_2O_2 (described below) or a mixture of 4g H_2SO_4:2g $(NH_4)_2SO_4$ was most suitable for dissolution. The H_2SO_4:$(NH_4)_2SO_4$ mixture can be used immediately after preparation while it is still hot and had the advantage of no gas evolution during or after the digestion process. For LLTO it was found that a mixture

of H_2SO_4:HNO_3:H_2O_2 was an ideal digestion these materials. An experimental matrix for each process is laid out in Table 1.

1) Wet chemical dissolution:

The simplest digestion process involves thermal activation by use of e.g., a hot plate or a sand bath. The temperature is limited by the boiling point of the digestion solution and typically means that the lower the temperature the longer the necessary digestion times.

Process 1a) entails adding the oxide powder to 15 mL polypropylene centrifuge tubes along with the commensurate digestion solution. The vials are then heated using a sand bath on a hot plate to at least 80°C for several days with the lids loosely adhered to avoid pressure build up. Digestion in this vessel is exceedingly slow but could be used as a control. Attempts to improve digestion through the use of a heated ultrasonic bath were unsuccessful.

Process 1b) involves the use of Parr Digestion Bombs (Type 4749) lined with Teflon vessels. Powders then liquids (10 mL) were added to the vessels and sealed to the recommended torque values. The vessels were heated in a laboratory-based oven to 135-150°C with 3 methods of evaluating the temperature (this was to avoid exceeding the operating pressure of the vessels as some of the reagents were quite volatile). This included the furnaces temperature control (coarsest control ± 25°C), an external thermocouple located next to the vessels, and single use thermal sensors (Omega Engineering TL-E-250 and -330).

Process 1c) utilizes the maximum temperature for the ammonium sulfide digestion solution, making it the fastest process. Sample aliquots of 50 mg were accurately weighed into quartz beakers at least in duplicate. 2 g ammonium sulfate (Suprapur 99.9999%, Sigma-Aldrich) and 4 mL sulfuric acid (Suprapur, Merck, Darmstadt, Germany) were added and the mixture was slowly heated on a hot plate using a magnetic stirrer. The temperature was gradually increased to the maximum temperature (about 250-300°C) until fuming. Note hood compatibility with fuming acids should be evaluated before this approach. Heating was continued until the sample was completely dissolved, typically after 2-3 hours. Afterwards the mixture was allowed to cool while stirring, then transferred to polypropylene tubes and made up to 50 mL with deionized water. Two replicate dilutions of each digestion solution were prepared at two levels: 200-fold and 10-fold.

2) Microwave assisted dissolution:

Process 2 involves the use of a CEM MARS 6 Microwave digestor with standard 50 mL Teflon vessels and active temperature monitoring. To each liner, finely ground powders were added followed by the slow addition of 10 mL of 1:1 volume of nitric and sulfuric acid. The solution was allowed to cool to room temperature. This cooling step was important to avoid excess decomposition of H_2O_2. After cooling, 2 mL of cold 30% H_2O_2 was added dropwise to the liner contents with subsequent gas evolution. After no further gas evolution was observed, the liner was then sealed and placed in a microwave digester at 260°C for 35

minutes (CEM MARS 6). The contents were allowed to cool and then diluted with deionized H_2O to 20 mL.

3) Thermal treatment for sulfide:

Sulfides were digested in a thermal process. Samples were weighed in an argon filled glove box and placed in small glass vials. The vials were loaded in a quartz tube with ultra torr type fittings with valves to isolate the samples from the moisture in the air. The quartz tube ensemble was removed from the glove box and connected to a dry air cylinder. The dry air was purged into the quartz tube and allowed to react for 24 hours. The samples were then heated to 400^{o}C in dry oxygen to form a sulfate. The use of dry air was essential to avoid the formation of volatile H_2S products. The sulfate was easily dissolved in aqua regia (3:1 HCl:HNO_3).(*18*)

Inductively coupled plasma optical emission spectroscopy (ICP-OES):

ICP-OES measurements were carried out on a Thermo Scientific iCAP 7400 ICP-OES Duo and iCAP 7600 (Thermo Fisher Scientific). An important source of error is the ICP standard solutions which are necessary for instrument calibration. Commercially available calibration standards pose an easy way to obtain suitable calibration curves. For the LLZO analysis, Calibration standards were prepared in the range from 0.05 mg L^{-1} to 4 mg L^{-1} from single element standards (Supelco/Merck, Darmstadt, Germany) with matrix matching of the digestion reagents. All calibration stock solutions did not contain HF. However, they have a very limited shelf life and thus lead to higher operation costs. A more cost-effective way for smaller laboratories is the preparation of the necessary calibration standards in house but offers the opportunity for errors in processing. Indeed, the transition metals are typically dissolved with a small amount of HF to act as a mineralizer. However, lanthanum ions readily coordinate with F^- forming LaF_3 as a precipitate. Thus. our approach involves preparing two sets of ICP standards: one for La and the other for the transition metals. To ensure reproducibility and check for instrument drift with time or solution aging Li, P, and Na were added to all of the standards and used as an internal control. As such a direct comparison between the two sets of standards (the La and the transition metals) can be made and drifts associated with sample aging can be identified. Calibration solutions were made with the digestion acids consisting of approximately 10 vol% in the mixture (not including H_2O_2 due to the volatility with time). Each data collection was collected in duplicate (or more) along with a 200:1 and a 10:1 dilution from the parent solution to ensure linearity and reproducibility.

Results and Discussion

During the course of our work on solid electrolytes it has become clear that composition values for the prepared solid electrolytes are lacking in the literature. Further, the addition of excess lithia precursors

is an almost universally accepted part of the manufacturing process with significant costs associated with the lost reagent. Additionally, the Li content in the final component or more exactly the amount of mobile Li and Li vacancies, determine the total ionic conductivity of the solid electrolyte. It was found for LLZO several years ago, that besides the crystal structure of the electrolyte the total Li content will have a strong effect on the total ionic conductivity.(*12*) While the Li loss mechanism is certainly the evaporation of Li during thermal treatment (sintering), the exact time after which the optimal Li concentration is reached depends on many experimental conditions which are often hard to control even with respect to reproducibility. Parameters like crucible material and age, oven type, temperature spread/offset and type of component (powder, thin sheet, bulk sample, etc.) can lead to large variations in Li content for similar experimental conditions which are typically reported in literature, namely ramp rate, maximum (set) temperature and dwell time. Therefore, it is necessary to carefully analyze the lithium content for each experimental setup, sample style, materials variation, and synthesis condition. To help with this essential task, we have developed a robust process to digest the oxide-based Li ion conducting ceramics to perform reliable elemental analysis via ICP-OES. Through the experimental procedure, and Table 1, we have explored a large number of reaction conditions for the digestion process with the goal of developing stable solutions with time suitable for reproducible ICP data collection.

Table 1. Attempts at digesting LLTO and LLZTO

Acids	Ratio (volume – unless noted)	Process 1	Process 2 – Parr	Process 3 - Microwave
HCl		Insoluble		Insoluble
$HCl:HNO_3$	3:1	Insoluble	TiO_2/ZrO_2 precipitate	
$HCl:HNO_3:HF$	3:1:1	White precipitate	LaF_3 precipitate	LaF_3 precipitate
HCl:oxalic acid	1:0.1		Insoluble	
$HNO_3:H_2SO_4$	1:1	LLTO slightly soluble, LLZO unreacted		
$HNO_3:H_2SO_4:H_2O_2$	1:1:0.2	Insoluble	Soluble	Soluble
$HNO_3:H_3PO_4:HF$				LaF_3 & phosphate precipitate
$HNO_3:HF$	10:0.5			LaF_3 precipitate
H_2SO_4		Insoluble	Insoluble	Insoluble
$H_2SO_4:(NH_4)_2SO_4$	4g:2g		Insoluble	LLTZO soluble/LLTO insoluble
$H_2SO_4:HCl$	5:3	Insoluble		Insoluble
$H_2SO_4:H_3PO_3$	1:1	Insoluble		
$H_2SO_4 :H_3BO_3$	3:0.17g	Insoluble	Insoluble	
$H_2SO_4:HNO_3:H_3BO_3$	2:1:0.1g	Insoluble		Insoluble
$H_2SO_4:H_2O_2$	5:1	Insoluble		Insoluble
$H_2SO_4:HNO_3:HF$	4:1.5:1.5			LaF_3 precipitate
$H_2SO_4:H_3BO_4:HF$	4:1.5g:3			La/Ti precipitate
$H_2SO_4:(NH_4)_2SO_4:HCl$	10:2:12			Ta_2O_5 precipitate
$H_2SO_4:(NH_4)_2SO_4:HF$	4g:2g:0.5mL	Insoluble – fluffy LaF_3		LaF_3 and Ta precipitate

First, to ensure proper calibration using self-prepared calibration standards, it was identified that any residual F^- from HF or metal fluorides readily reacts with aqueous La^{3+} and results in the precipitation of LaF_3. The size of the LaF_3 precipitates depend on the concentration of F^- and are often hard to observe with well shaken solutions.

Figure 1 (top) shows La ICP data collected for samples mixed with Ti, Ta, and Zr ICP solutions as part of a standards preparation [• data points] after 3 weeks of aging. The data appears deceptively linear and would indicate a low sensitivity to La. However, this is misleading as the signal decreases with time due to the aforementioned precipitation reaction. When a calibration curve is made without trace F^- [■ data points] the curve remains constant and shows excellent sensitivity to La following Beer's Law of adsorption.

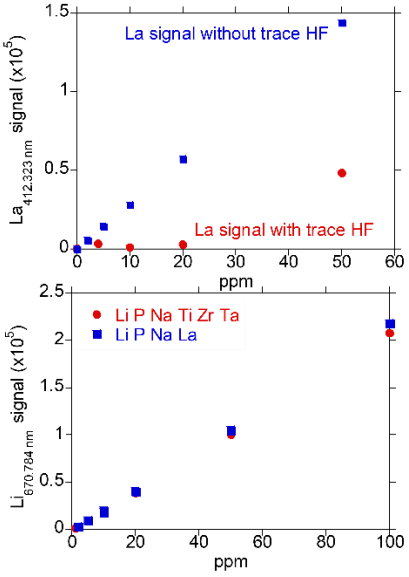

Figure 1. Top – La ICP signal versus concentration for standards with (blue square) and without (red circle) trace HF; Bottom - Li ICP signal versus concentration for standards with Li, P, Na and La (blue square) and with Li, P, Na, Ti, Zr, Ta (red circle) and trace HF. The P and Na are internal standards to look for deviations in mixed matrix standards.

Following this observation, we developed procedures where two sets of standards were produced. One set of standards was focused on La, the second sets contained the transition metals (which are generally dissolved with trace HF). To ensure translation between the standards fixed concentrations of Li, P, and Na were added to ensure a direct comparison between the samples and check for sample or instrument drift. Figure 1 (bottom) shows representative Li ICP data from these various standards. Again, the data shows a linear Beer's Law relationship along with small errors between different solutions.

Second, the impact of the digestion solution was investigated. From our experiments we identified a reaction mixture that would dissolve Li-La-Ti-O and Li-La-Zr-Ta-O solid electrolytes (H_2SO_4:HNO_3:H_2O_2) and a second solution (H_2SO_4:$(NH_4)_2SO_4$) that would dissolve Li-La-Zr-Ta-O based materials. The H_2SO_4:$(NH_4)_2SO_4$ was reported once before in the literature through heating the mixture to boiling (337ºC).(*19*) LLZO has also been reported digested at 1000ºC with boron-oxide flux and dissolution with HF.(*20*) Prior LLTO work reported the use of HCl and heating to 130ºC or HCl+H_2O_2+heat to dissolve LLTO. We found HCl to be ineffective and prone to produce dilute TiO_2 materials with exposure to oxidation. It is possible that the difference could be related to either the mass of sample, as the literature samples were thin films, or the fact that the thin films were amorphous films while our samples were bulk, crystalline material.(*21, 22*) Through the use of pressure vessels, the volatile HNO_3 and H_2O_2 could be contained. Second, the use of H_2SO_4 is hypothesized to produce a soluble SO_4^{2-} based species suitable for the ICP analysis. It is unclear why the $(NH_4)_2SO_4$ solutions promote the dissolution of the LLZO samples though we hypothesize this is due to the formation of an ammonium complex with the Zr or Ta that is not formed with Ti. After the digestions it was observed that the solutions became a distinctive yellow/orange color, Figure 2. Upon addition of water the orange solution immediately turned a green color (Figure 2 center) and began to evolve a noxious orange gas (NO_x), Figure 3. While the solution is still green, agitation and mixing with the air appeared to increase evolution of the orange gas. Agitating the solution in a sealed tube also evolved orange gas, but it is interesting that the tube did not noticeably pressurize, indicating that the orange gas may be a reaction that is consuming oxygen; the consumption of oxygen would result in a net zero gas production thus preventing pressurization. The generation of gas does not affect the species in solution. After 24 hours the sample resulted in a clear, colorless solution that was stable for weeks and suitable for ICP analysis.

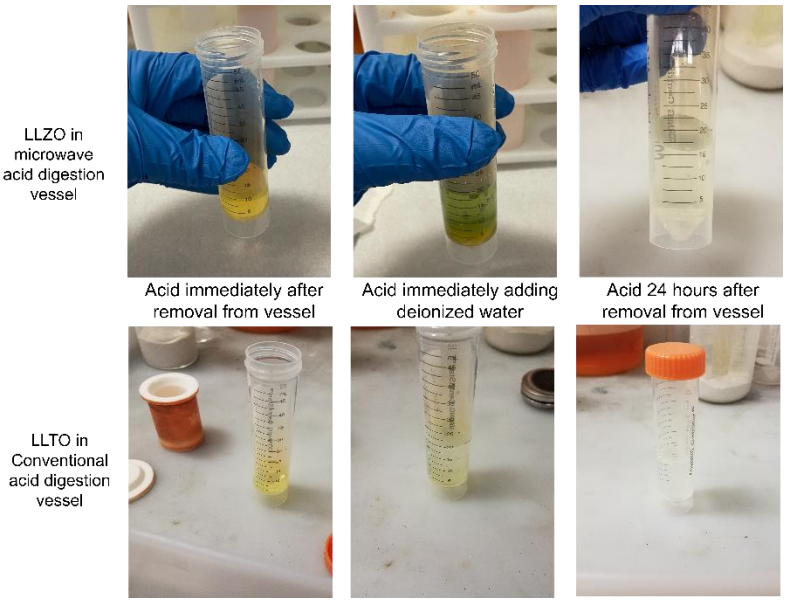

Figure 2. Images of digestion mixture after removal from vessel (left), addition of deionized water (center) and after aging (left) for LLZO (top) and LLTO (bottom).

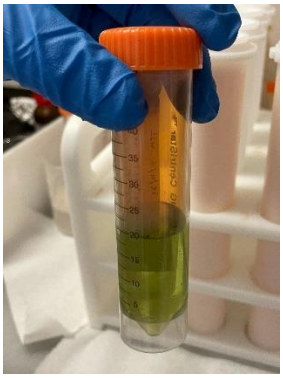

Figure 3. Image of microwave digested LLTZO in H_2SO_4:HNO_3:H_2O_2 showing orange gas evolved.

For LLTO solid electrolytes stoichiometric $Li_{0.3}La_{0.57}TiO_3$ starting material were used in these experiments. These materials were prepared using Li_2O_2, LiOH, $LiNO_3$ and Li_2CO_3 precursors which have different decomposition temperatures (340, 467, 485, 728°C – respectively). X-ray diffraction data for the starting material are shown in Figure 4. The LLTO materials were single phase while commercial samples had small impurities from $La_2Ti_2O_7$ and $LiTi_2O_4$. Further, the samples were prepared in a standard solid-state reaction with lithium source, La_2O_3 and TiO_2 or with prereacted La_2O_3 and TiO_2 forming $La_{0.57}TiO_{2.855}$ that the Li source was added and subsequently reacted.(*17*) The ICP data shows using the standard solid state reaction at 1000°C the lithium losses were within error of the measurement or about 0.01 moles of Li (versus the starting 0.30 moles of Li), Figure 5 (top). Heating to 1200°C shows clear losses from the LiOH precursor (0.05 moles versus starting value of 0.3 moles of Li). Clearly the addition of 20% excess LiOH for a reaction at 1200°C is warranted but for samples annealed at 1000°C excess Li-precursor would not be required to obtain the desired composition. We note these are absolute numbers since the total concentration of Li, La, and Ti were obtained.

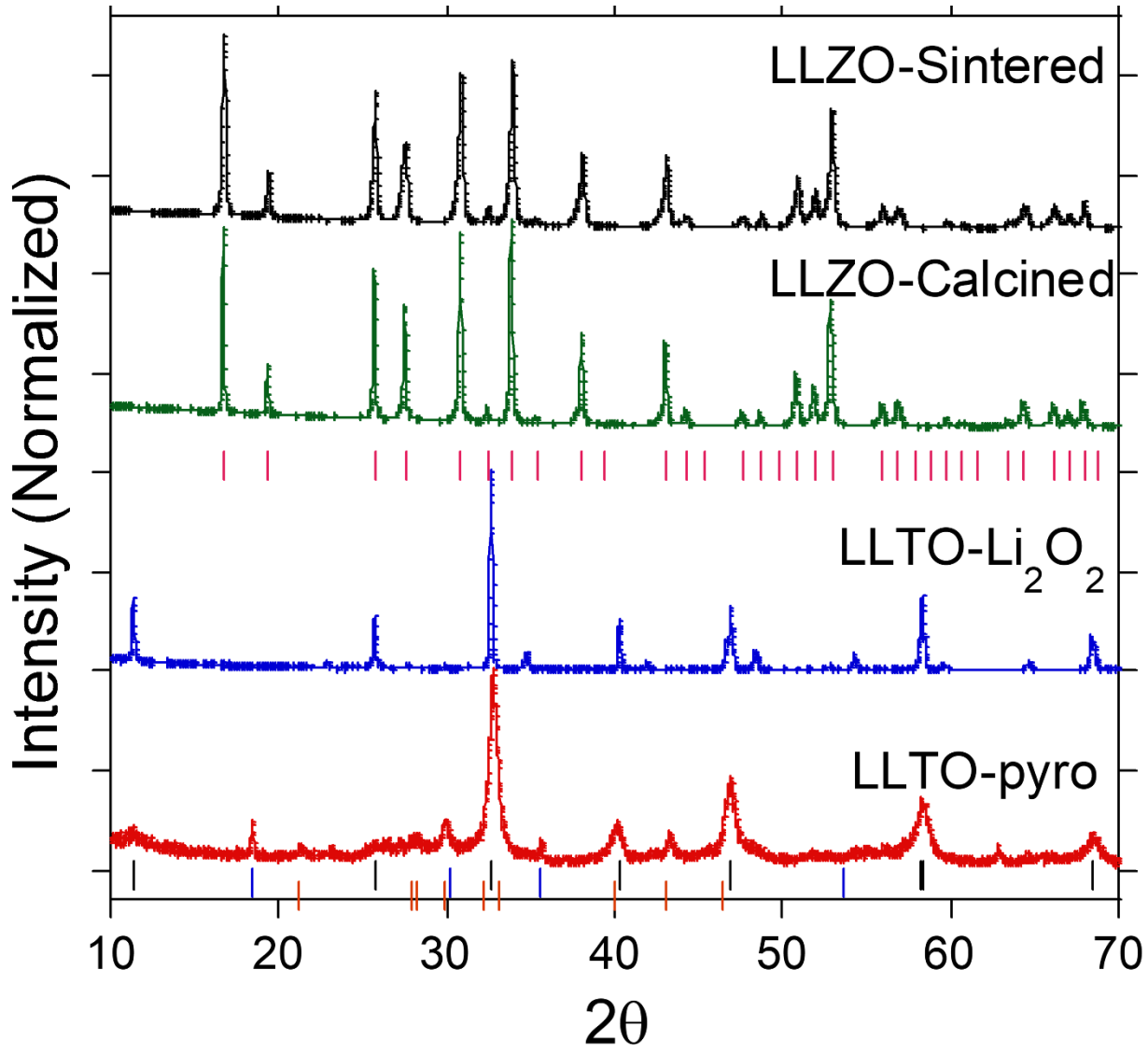

Figure 4. Powder X-ray diffraction data of the materials used to develop the procedures (bottom) and representative research quality samples of LLTO from Li_2O_2 precursor, calcined LLZO and sintered LLZO. The vertical markers indicate peaks associated with LLZO (pink), LLTO (black), $LiTi_2O_4$ (blue), and $La_2Ti_2O_7$ (red).

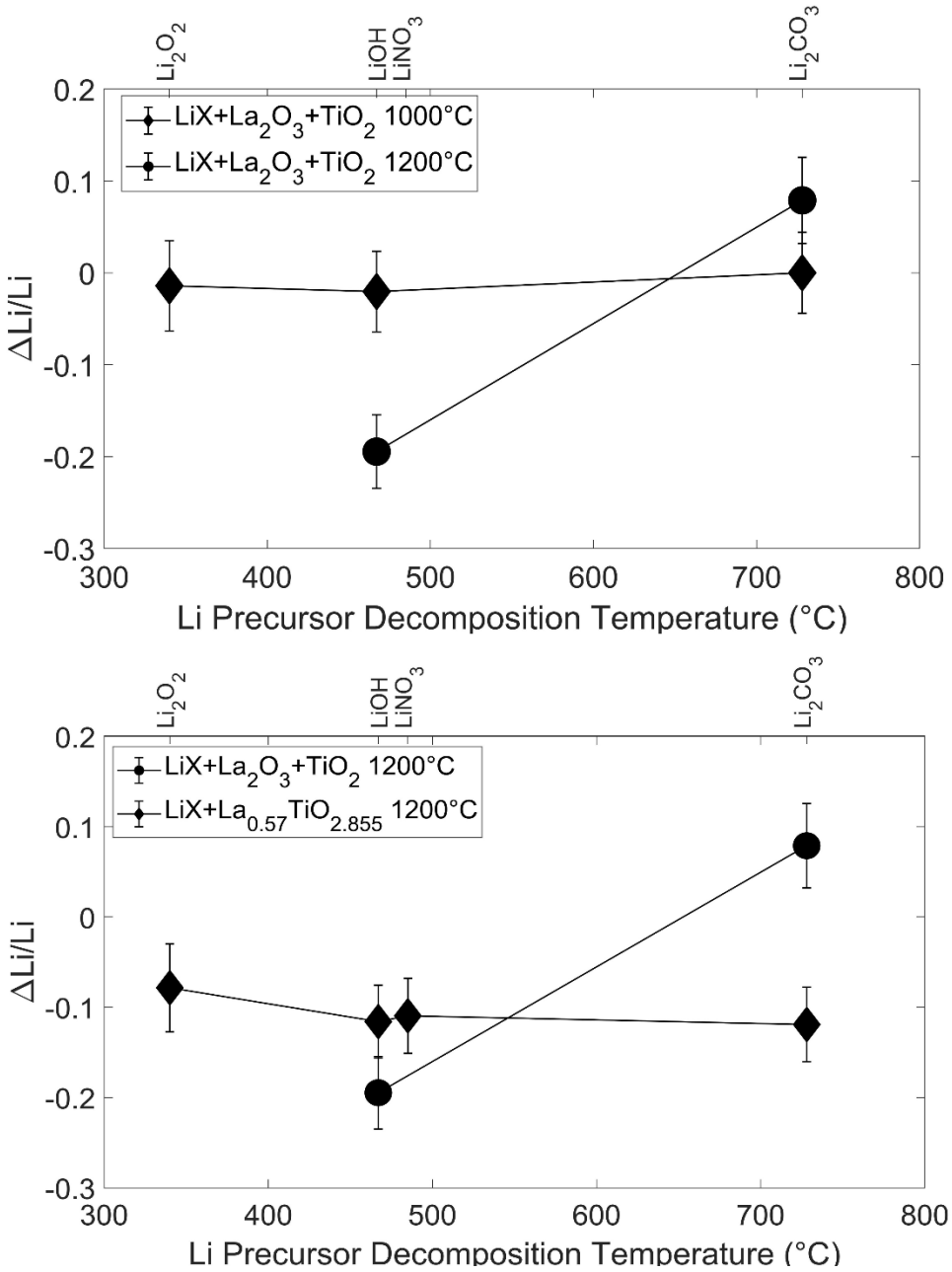

Figure 5 (top) Change in Li content as a function of lithium precursor decomposition temperature for samples annealed at 1000 and 1200°C (top) and through varying the orders of addition (bottom).

Data from the second reaction involving the addition of Li-precursor to $La_{0.57}TiO_{2.855}$ is presented in Figure 5 (bottom). From this analysis the losses of lithium appear to grow in magnitude with Li-precursor decomposition temperature. However, under these conditions the losses are around 0.03 moles Li (10%). Clearly the addition of 20% excess Li-precursor would be a waste to obtain the pure $Li_{0.3}La_{0.57}TiO_3$.

For LLZO a large variation of synthesis processes can be found in literature, with typical, industrial viable processes being described in our previous work.(*16*) In almost all cases, an excess of 20 mol % with respect to the stoichiometric final composition is used. The powders used in this study were synthesized by conventional solid-state reaction (SSR) and have a nominal composition of $Li_{6.4}Al_{0.2}La_3Zr_2O_{12}$ (LLZO:Al) and $Li_{0.645}Al_{0.05}La_3Zr_{1.6}Ta_{0.4}O_{12}$ (LLZ:Ta) and were analyzed in two major states of processing, once after the third calcination step of the powder at 1000°C and again after the sintering of the pellet at 1200°C and 1175°C respectively.

To test the robustness of the digestion procedure 1c), the digestion time and temperature was varied, and the respective elemental concentration determined and compiled in Table 2. The values were normalized to the expected Zr+Hf value of 2.0 for LLZO:Al and 1.6 for LLZO:Ta respectively. The calculated standard deviation from the expected stoichiometric value for the samples are given as "SD from ICP" in the last column.

Most interestingly, the digestion process is rather robust in the test regime, with both 200°C and 350°C resulting in complete dissolution after 2-3 h on the hot plate. The standard deviation calculated from is low, typically in the 1-2% range. However, with respect to the target stoichiometry, the variation is much larger, especially for La. From a synthesis point of view, the typical error is a La sub-stoichiometry due to insufficient drying of La_2O_3 prior to the weigh in procedure. In contrast, the used ICP-OES analysis always overestimates the La content by about 10% compared to the expected stoichiometry. Further, concentrations of water or carbonate are unlikely to vary by 10 wt% during robust drying processes. The reason is elusive so far, possibly originates in the sensitivity of the dissolved La in the calibration standards to HF; this risk was minimized by applying commercial calibration standards without HF.

Thus, normalization to the Zr and/or B site dopants is proposed to obtain a robust analysis of Li and other heavy elements. For Li, similar to the observations made for LLTO, the Li content changes little from the expected 7.8 in the starting material upon calcination, even after a total of 50 h at 850-1100°C. The main Li loss occurs after sintering at 1200 °C, reducing the Li amount to almost the stoichiometric value for LLZO:Al after another 30 h. After 10 h at 1175°C for LLZO:Ta, the Li content is still at approx. 10 % excess, even though the LLZO:Ta samples typically already show rather high total ionic conductivities. Additionally, as known from literature, the sample takes up a large amount of Al from the Al_2O_3 crucible. This demonstrates the necessity to closely monitor the dopant concentration as well as the Li content to tailor the stoichiometry for optimal electrochemical performance.

Table 2: Variation in elemental composition of Al doped LLZO (LLZO:Al) and Ta +Al substituted LLZO (Ta:LLZO) after calcination and after sintering for 3 variations of dissolution process 1c).

Sample	200°C for 3h	350°C for 2h	350°C for 4h	SD from ICP	Deviation to expected stoichiometry
LLZO:Al calcined					
Li	7.37	7.31	7.39	2%	
La	3.27	3.26	3.27	2%	8.8 %
Zr	1.98	1.98	1.98	1%	
Ta	0.00	0.00	0.00	1%	
Al	0.18	0.19	0.19	0%	
Hf	0.02	0.02	0.02	2%	
LLZO:Al sintered					
Li	6.79	6.73	6.88	1%	
La	3.20	3.18	3.17	3%	6.1 %
Zr	1.98	1.98	1.98	1%	
Ta	0.00	0.00	0.00	1%	
Al	0.17	0.17	0.17	0%	
Hf	0.02	0.02	0.02	3%	
LLZO:Ta clacined					
Li	7.89	7.82	7.84	2%	
La	3.31	3.29	3.29	2%	9.9 %
Zr	1.58	1.58	1.58	2%	
Ta	0.42	0.41	0.41	2%	3.6 %
Al	0.14	0.14	0.14	3%	
Hf	0.02	0.02	0.02	1%	
LLZO:Ta sintered					
Li	7.26	7.13	7.16	2%	
La	3.41	3.39	3.40	2%	13.3 %
Zr	1.58	1.58	1.58	1%	
Ta	0.43	0.42	0.42	1%	6.0 %
Al	0.12	0.11	0.12	1%	
Hf	0.02	0.02	0.02	2%	

To investigate if the synthesis method has an effect on the dissolution process, calcined powders from two wet chemical synthesis routes, solution assisted solid state reaction (SA-SSR) and spray drying (SD),(*16*) were investigated and compared to the conventional SSR. Interestingly, the SA-SSR provides much better mixing of the precursor materials and rather large primary particles after calcination, shows a similar over-estimation of the La content by ICP-OES as the SSR sample. In contrast, the SD sample featuring mixing on atomic scale of the precursors and very small particle sizes has less over-estimation of the La content. However, for Li and Al the results are reasonable and show the expected Al and Li concentration after calcination. As trivial as this result might seem, it ensures the chemical comparability of the powders from both synthesis processes and allows the discernment of possible variations in electrochemical performance

of a final battery component from these powders to other factors like particle size, morphology, post treatment (surface conditioning) or the manufacturing process itself. It is thus a vital part of ensuring the scientific quality of the obtained results and improves reproducibility of the published work.

Table 3: ICP-OES results for 3 different synthesis methods of LLZO:Al using digestion method 1c)

Element	LLZO:Al SSR	LLZO:Al SA-SSR	LLZO:Al SD
Li	7.31	7.39	7.50
La	3.26	3.27	3.02
Zr	1.98	1.98	1.98
Ta	0.00	0.00	0.00
Al	0.19	0.19	0.18
Hf	0.02	0.02	-

Conclusion:

In this work we demonstrate several approaches to digest solid electrolyte materials and quantitatively analyze the constituent atoms. Such elemental analysis is critical to advancing the field of solid electrolytes and all solid-state batteries where structure-property correlations are highly dependent on vacancy concentrations and lithium stoichiometry. We recommend extensive efforts to evaluate La stability in solutions and in the case of LLZO normalization of content to the Zr species. Given the availability of these results we recommend researchers incorporate these approaches to advance the field beyond Edisonian heat-and-beat synthesis work.

Acknowledgement:

The authors would like to thank Dr. Tim Armstrong (Steward Advanced Materials - Chattanooga TN) for the commercial samples of solid electrolytes. GMV would like to thank Diana Stamberga in ORNL's Chemical Separations Group for repeated access to the ICP used in this work and the high level of safety instilled in her laboratories. Work at ORNL (TFM, EOB, GMV – LLTO, LLZO digestion, Na_2S) was supported by the U.S. Department of Energy, Office of Science, Basic Energy Sciences, Materials Science and Engineering. Work at Julich was conducted as part of the US-German joint collaboration on "Interfaces and Interphases In Rechargeable Li-metal based Batteries" supported by the US Department of Energy (DOE) and German Federal Ministry of Education and Research (BMBF). Financial support from the BMBF within 03XP0223A. Additionally, funding from the German Federal Ministry of Education and Research (BMBF) under grant no.: 13XP0173A (FestBatt-Oxide) and 13XP0434A (FB2-Oxide) is gratefully acknowledged. This manuscript has been authored by UT-Battelle, LLC, under contract DE-AC05-00OR22725 with the US Department of Energy (DOE).

References

1. M. Abreu-Sepúlveda *et al.*, (2016) Synthesis and characterization of substituted garnet and perovskite-based lithium-ion conducting solid electrolytes. Ionics 22: 317-325.
2. T. Okumura *et al.*, (2011) Improvement of lithium ion conductivity for A-site disordered lithium lanthanum titanate perovskite oxides by fluoride ion substitution. J. Mater. Chem. 21: 10061-10068.
3. X. Han *et al.*, (2017) Negating interfacial impedance in garnet-based solid-state Li metal batteries. Nat. Mater 16: 572-579.
4. S. Narayanan, G. T. Hitz, E. D. Wachsman, V. Thangadurai, (2015) Effect of Excess Li on the Structural and Electrical Properties of Garnet-Type $Li_6La_3Ta_{1.5}Y_{0.5}O_{12}$. J. Electrochem. Soc. 162: A1772-A1777.
5. V. Thangadurai, W. Weppner, (2005) $Li_6ALa_2Ta_2O_{12}$ (A = Sr, Ba): Novel Garnet-Like Oxides for Fast Lithium Ion Conduction. Adv. Funct. Mater. 15: 107-112.
6. Z. D. Gordon, T. Yang, G. B. Gomes Morgado, C. K. Chan, (2016) Preparation of Nano- and Microstructured Garnet $Li_7La_3Zr_2O_{12}$ Solid Electrolytes for Li-Ion Batteries via Cellulose Templating. ACS Sus. Chem. & Eng. 4: 6391-6398.
7. Y. Shimonishi *et al.*, (2011) Synthesis of garnet-type $Li_{7-x}La_3Zr_2O_{12-1/2x}$ and its stability in aqueous solutions. Solid State Ionics 183: 48-53.
8. T. Thompson *et al.*, (2015) A Tale of Two Sites: On Defining the Carrier Concentration in Garnet-Based Ionic Conductors for Advanced Li Batteries. Adv. Energy Mater. 5: 1500096.
9. H. Buschmann, S. Berendts, B. Mogwitz, J. Janek, (2012) Lithium metal electrode kinetics and ionic conductivity of the solid lithium ion conductors "$Li_7La_3Zr_2O_{12}$" and $Li_{7-x}La_3Zr_{2-x}Ta_xO_{12}$ with garnet-type structure. J. Power Sources 206: 236-244.
10. R. Wagner *et al.*, (2016) Crystal Structure of Garnet-Related Li-Ion Conductor $Li_{7-3x}Ga_xLa_3Zr_2O_{12}$: Fast Li-Ion Conduction Caused by a Different Cubic Modification? Chem. Mater. 28: 1861-1871.
11. J. L. Allen, J. Wolfenstine, E. Rangasamy, J. Sakamoto, (2012) Effect of substitution (Ta, Al, Ga) on the conductivity of $Li_7La_3Zr_2O_{12}$. J. Power Sources 206: 315-319.
12. C.-L. Tsai *et al.*, (2015) High conductivity of mixed phase Al-substituted $Li_7La_3Zr_2O_{12}$. J. Electroceram. 35: 25-32.
13. E. Rangasamy, J. Wolfenstine, J. Allen, J. Sakamoto, (2013) The effect of 24c-site (A) cation substitution on the tetragonal–cubic phase transition in $Li_{7-x}La_{3-x}A_xZr_2O_{12}$ garnet-based ceramic electrolyte. J. Power Sources 230: 261-266.
14. H. Ohta *et al.*, (2012) Lithium-ion conducting $La_{2/3-x}Li_{3x}TiO_3$ solid electrolyte thin films with stepped and terraced surfaces. Appl. Phys. Let. 100: 173107.
15. R. Pfenninger, M. Struzik, I. Garbayo, E. Stilp, J. L. M. Rupp, (2019) A low ride on processing temperature for fast lithium conduction in garnet solid-state battery films. Nat. Energy. 4: 475-483.
16. M. Mann *et al.*, (2021) Evaluation of Scalable Synthesis Methods for Aluminum-Substituted $Li_7La_3Zr_2O_{12}$ Solid Electrolytes. Materials 14: 6809.
17. T. F. Malkowski *et al.*, (2021) Role of Pairwise Reactions on the Synthesis of $Li_{0.3}La_{0.57}TiO_3$ and the Resulting Structure–Property Correlations. Inorg. Chem. 60: 14831-14843.
18. R. D. McAuliffe *et al.*, (2021) Synthesis of Model Sodium Sulfide Films. *Submitted - J. Mater. Chem C.*

19. C.-L. Tsai *et al.*, (2016) $Li_7La_3Zr_2O_{12}$ Interface Modification for Li Dendrite Prevention. ACS Appl. Mater. Interfaces 8: 10617-10626.
20. P. Badami *et al.*, (2020) Highly Conductive Garnet-Type Electrolytes: Access to $Li_{6.5}La_3Zr_{1.5}Ta_{0.5}O_{12}$ Prepared by Molten Salt and Solid-State Methods. ACS Appl. Mater. Interfaces 12: 48580-48590.
21. Z. Zheng, Y. Zhang, S. Song, Y. Wang, (2017) Sol–gel-processed amorphous inorganic lithium ion electrolyte thin films: sol chemistry. RSC Adv. 7: 30160-30165.
22. Z. Zheng, S. Song, Y. Wang, (2016) Sol-gel-processed amorphous lithium ion electrolyte thin films: Structural evolution, theoretical considerations, and ion transport processes. Solid State Ion. 287: 60-70.